

Article

Prospects for Power Generation of the Doublet Supercritical Geothermal System in Reykjanes Geothermal Field, Iceland

Yu Wang¹, Tianfu Xu¹, Yuxiang Cheng^{1,2} and Guanhong Feng^{1,*} 

¹ Key Laboratory of Groundwater Resources and Environment, Ministry of Education, Jilin University, Changchun 130021, China

² Engineering Research Center of Geothermal Resources Development Technology and Equipment, Ministry of Education, Jilin University, Changchun 130026, China

* Correspondence: guanhong_feng@jlu.edu.cn

Abstract: Supercritical geothermal resources are in the preliminary exploration stage as a new type of clean energy and there are no practical utilization projects. The IDDP-2 well at Reykjanes geothermal field in Iceland encountered supercritical geothermal conditions in 2017, with a maximum temperature of 535 °C. The system is still in the field experiment stage and no exploitation work has been carried out. Hence, a hypothetical doublet geothermal system was simulated based on IDDP-2 to study the power generation potential and favorable operating conditions for future development of supercritical geothermal resources. A multiphase flow model is established to predict the fluid and heat flow characteristics. Furthermore, sensitivity and economic analyses were performed to evaluate the expected commercial and environmental benefits of the supercritical geothermal system. The results show that the system's evolution could be briefly divided into three stages according to the temperature variation. The power generation ranges between 5.4 MW~16.5 MW, and the levelized cost of electricity (LCOE) is 0.02 \$/kWh. In addition, the system can reduce CO₂ emissions, which are 1.2~7.75 Mt less than that of fossil fuel plants with the same installed capacity. The results prove the great development potential and commercial competitiveness of the supercritical geothermal system.

Keywords: supercritical geothermal; power generation; sustainability; IDDP-2 of Iceland



Citation: Wang, Y.; Xu, T.; Cheng, Y.; Feng, G. Prospects for Power Generation of the Doublet Supercritical Geothermal System in Reykjanes Geothermal Field, Iceland. *Energies* **2022**, *15*, 8466. <https://doi.org/10.3390/en15228466>

Academic Editors: Li Chen, Xiaoying Zhang and Feifei Qin

Received: 30 July 2022

Accepted: 20 October 2022

Published: 12 November 2022

Publisher's Note: MDPI stays neutral with regard to jurisdictional claims in published maps and institutional affiliations.



Copyright: © 2022 by the authors. Licensee MDPI, Basel, Switzerland. This article is an open access article distributed under the terms and conditions of the Creative Commons Attribution (CC BY) license (<https://creativecommons.org/licenses/by/4.0/>).

1. Introduction

With growing concern about the environmental impacts of climate change, there is a growing call to reduce the use of fossil fuels [1]. Currently, many countries worldwide are trying to adjust their strategic energy structure toward being more diversified, green, and low carbon. Renewable energy is gradually being valued as an environmentally friendly green energy source. According to the renewable energy statistics 2020 of the International Renewable Energy Agency (IRENA), the amount of electricity generated from renewable energy was 2.47×10^{16} J in 2018 (<https://irena.org/publications/2020/Jul/Renewable-energy-statistics-2020>, accessed on 2 July 2019).

Among all sorts of renewable energy resources, geothermal energy is widely distributed, low carbon, and safe. Supercritical geothermal is an emerging type of geothermal resource, which refers to the P, T condition beyond the critical point of the heat transmission fluid, typically such as water (374 °C, 22.1 MPa). Compared with traditional geothermal resources, supercritical water possesses the characteristics of high specific enthalpy and low viscosity, which is advantageous for heat extraction. Therefore, many countries have conducted relevant research on exploring, drilling, and developing supercritical geothermal resources, including the IDDP in Iceland, Newberry and Salton Sea in the United States, DESCRAMBLE in Italy, and JBBP in Japan. However, it is still in the preliminary exploration stage and commercial development has not been achieved.

Among them, the sites in Iceland and Italy have made rapid progress in drilling and field experiments [2]. The Iceland Deep Drilling Project (IDDP) was mainly launched in the

early 21st century to find suitable sites of 450–600 °C conditions at 3.5–5 km underground to achieve economic development [3,4]. The IDDP-2 well started in December 2015, based on an existing borehole RN-15 with a depth of 2500 m, and was completed in January 2017. The depth of the well is 4659 m and 4500 m vertically. The trajectory of the well is inclined to the southwest below 2750 m [5]. The bottom hole temperature is 535 °C [6], which meets the supercritical conditions. After the completion of the IDDP-2 well, several injection tests were carried out to evaluate the injectivity and hydrogeological properties of the reservoir [5]. According to the P-T measurements, they found three highly permeable reservoirs below 3000 m depth, with depths of 3400 m, 4300 m, and 4500 m.

The Reykjanes geothermal field is located in the southwestern part of the Reykjanes Peninsula, Iceland. The volcanic coverage area is about 25 km². Its position is transitional between the Reykjanes Peninsula's trans-tensional plate boundary and that of the Reykjanes Ridge of primarily extensional structure [7]. There is a total of 34 drill holes, which can supply steam to a 100 MWe power plant from a 300 °C reservoir at 1000 to 2500 m depth [8]. The lithology of the Reykjanes Peninsula can be divided into two parts. The upper part (above ~1400 m depth) mainly contains volcanic rock with interbedded zones of basalt flows, pillow lavas, and hyaloclastite. The lower part (below ~3500 m depth) is the sheeted dike complex [8,9]. The zone between 1400 and 3500 m is the transition zone. According to Cladouhos et al. [10], the heat extraction rate at 400 °C can reach 50 MW at a mass flow rate of 60 kg/s, which is approximately 10-fold the heat extraction efficiency of liquid water at 200 °C. Their study also showed that it requires 18 injection wells and 23 production wells, covering an area of 30 km² at a flow rate of 85 kg/s, for a conventional geothermal system (200 °C) to generate 120 MW power. Whereas for a 400 °C supercritical geothermal system, it only needs one injection and two production wells, covering an area of 1 km², which can generate 106 MW of power at a flow rate of 60 kg/s.

Numerical simulation is a convenient and effective method to predict and optimize the operating conditions of a geothermal system. However, these investigations above are based on ultra-simplified models, not focusing on any specific geothermal site. The reason for this is that the description of multiphase flow in supercritical conditions is still a challenge for numerical simulations. There is no mature commercial software that can handle supercritical conditions and most academic programs are in the in-house testing stage. This study adopts the program developed by Feng et al. [11,12]. Given the current development status of supercritical geothermal resources—there is only one IDDP-2 well completed—the candidate well to be deepened and combined with IDDP-2 to form a geothermal doublet has not been determined. Hence, it is significant to evaluate the development potential and economic and environmental benefits of the supercritical geothermal system. The wellbore layout, operating conditions, etc., all need to be properly designed to maximize the geothermal development.

2. Materials & Methods

2.1. Model Setup

A doublet geothermal system was simulated for the development of supercritical geothermal resources to study the power generation performance based on the IDDP-2 conditions. Although the permeability of the upper layer is higher, it is more likely to be a large fracture zone and its boundary is not clear, which may cause most of the injected fluid to be lost. Therefore, the reservoir selected for this study is the lowest layer with the highest temperature at a depth of 4500 m.

In order to simplify the model and to improve the calculation efficiency, the low-permeability confining formation is not considered, and the heat exchange between these formations with the reservoir and wellbore is taken into account by specific semi-analytical solutions. The mesh for the simulation is shown in Figure 1. According to the drilling trajectory, the angle between the borehole below 2750 m and vertical is about 23°. The thickness of the reservoir is assumed to be 50 m. The lateral boundary is set to 10 km, which is sufficient to eliminate the influence of lateral flow. In order to properly capture the

heat transfer process and fluid flow in detail, the spatial discretization in the vicinity of the wellbores is refined [13–15], and the size of the gridblock gradually becomes larger away from the wellbores to improve the calculation efficiency.

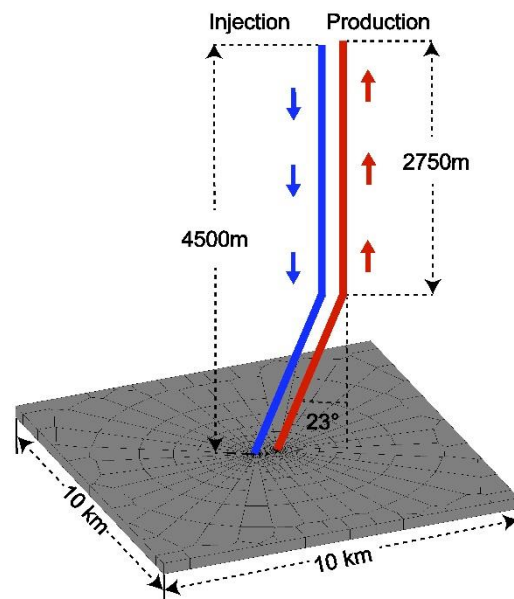


Figure 1. Sketch of the doublet supercritical geothermal system based on IDDP-2 (the reservoir thickness is 50 m).

Constant cold-water injection could stimulate the reservoir to enhance its permeability and injectivity. According to the injection test, the injectivity of the reservoir increases from 1.71 kg/s/bar to 3.11 kg/s/bar in less than one month. Hence, it is feasible to realize commercial development for IDDP-2 in the future. In this work, the reservoir is assumed to be homogeneous with a permeability of 50 mD.

Hokstad and Tanavsuu-Milkeviciene [16] combined the gravity and electromagnetic measurement data of the well to predict the initial temperature and pressure conditions of the reservoir. The temperature of the reservoir is set to 500 °C. Under hydrostatic conditions, the pressure is about 25.2 MPa. The mass flow rate for production is 25 kg/s. Due to the phase change from the in-situ high-temperature steam to water, some more water is required to be injected for pressure balance (it will be discussed later). Here, an extra 10% is given, i.e., 27.5 kg/s for injection with a temperature of 60 °C. Other thermo-physical parameters are shown in Table 1. In this work, the numerical simulation program used is TOUGH2-scESO1 developed by Feng et al. [11] based on the TOUGH2 code.

Table 1. Thermo-physical parameters and initial/boundary conditions for the numerical simulation.

Reservoir Formation	
Density	2700 kg/m ³
Specific heat capacity	900 J/(kg·°C)
Porosity	0.05
Thickness	50 m
Wellbore Diameter	0.1778 m
Roughness	10 ⁻⁵ m
Well spacing	600 m
Initial/Boundary condition	
Reservoir pressure	25.20 MPa
Reservoir temperature	500 °C
Injection temperature	60 °C
Production mass flow rate	25 kg/s
Injection mass flow rate	27.5 kg/s

2.2. Performance Criteria

The development of geothermal energy generally focuses on the production temperature and flow rate [17–19]. However, it is not accurate to evaluate the power generation potential of the geothermal system based on these alone. Therefore, in this work, the output temperature, flow rate, power generation, energy efficiency, and economic and environmental benefits have been comprehensively considered.

During the development of geothermal resources, the produced high-temperature steam cannot be directly converted into electrical energy. It is a two-step process; first from thermal to mechanical, and then to electricity. The net heat flow (W_h) is calculated according to the formula in Pruess [20], as Equation (1)

$$W_h = Q_{pro}(h_{pro} - h_{inj}) \quad (1)$$

where Q_{pro} is the production mass flow rate and h_{pro} and h_{inj} are the specific enthalpy of production and injection fluid.

The conversion efficiency (f_1) from thermal to mechanical energy is proportional to the production temperature. According to the second law of thermodynamics, the conversion efficiency (f_1) could be calculated as Equation (2)

$$f_1 = 1 - (T_{inj}/T_{pro}) \quad (2)$$

where T_{pro} and T_{inj} are the temperature of production and injection water.

In the process of converting mechanical energy to electrical energy, the maximum efficiency (f_2) is 0.45 [21]. Therefore, the conversion efficiency from thermal to electricity (f) could be calculated as Equation (3)

$$f = f_1 \times f_2 = 0.45 - 0.45(T_{inj}/T_{pro}) \quad (3)$$

and the power generation (W_e) could be calculated as Equation (4):

$$W_e = fW_h \quad (4)$$

In addition, energy efficiency (η_e) is also an important parameter in the process of power generation, which is the ratio of power generation (W_e) to energy consumption (W_p) [22], as Equation (5). The energy consumption is mainly caused by injection and production well pumps. The higher the energy efficiency, the better the economic benefits. The energy consumption calculation process of the pump is as follows:

$$\eta_e = W_e/W_p \quad (5)$$

$$W_{p1} = qP_{inj}/\rho\eta_P \quad (6)$$

$$W_{p2} = qP_{pro}/\rho\eta_P \quad (7)$$

$$W_p = W_{p1} + W_{p2} \quad (8)$$

where W_p is the consumption energy of the pump and the subscripts 1 and 2 represent production and injection well, respectively. P is the pressure at the wellhead. ρ is the fluid density. η_P is the pump efficiency. According to previous studies, the value is 80% [23].

3. Results

3.1. Fluid and Heat Flow

3.1.1. P/T Distribution in the Reservoir

At first, the same mass flow rate is given for both injection and production as the experience in the traditional geothermal system applications. However, after several simulation trials, it is found that the scheme of the same mass rate is inapplicable. The pressure distribution at different times is shown in Figure 2. It can be seen that the pressure

keeps decreasing over the whole area and it has dropped by nearly 3 MPa around the production well. This is attributed to the condensing of the in-situ supercritical fluid. An equivalent mass flow rate for both injection and production will bring a constant reduction of the pore pressure. It will cause mechanical damage to the reservoir for a long-term operation, which is not conducive to sustainable development and utilization.

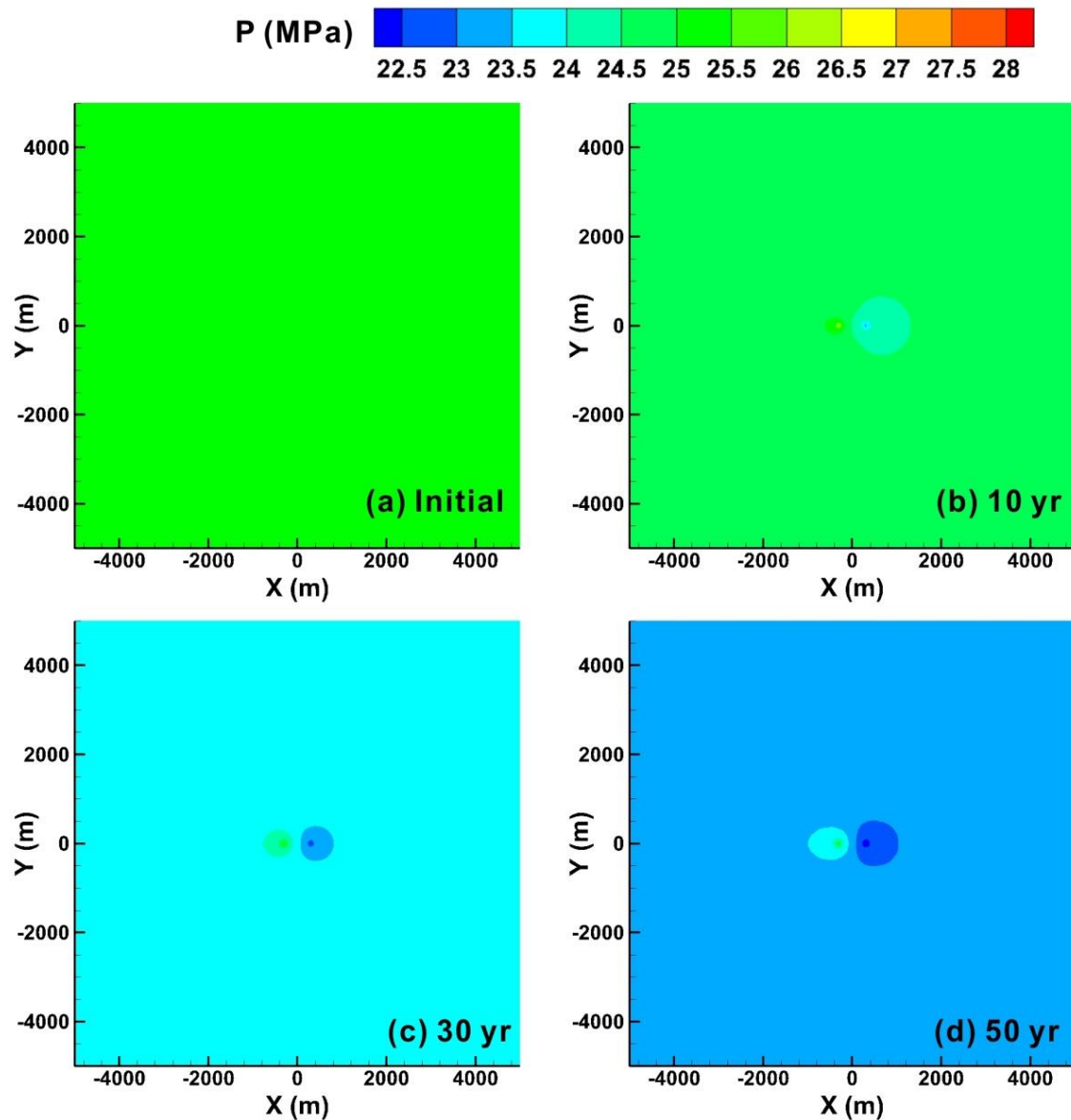


Figure 2. The reservoir pressure distribution at different times with the scheme of the same mass flow rate for injection and production.

Therefore, we proposed a compensatory injection scheme with a higher mass rate for injection than the production, which will keep the reservoir pressure stable. It is found that an extra 10% injection amount is effective in maintaining the reservoir pressure in fifty years of operation (as shown in Figure 3). Thus, the scheme of 27.5 kg/s for injection and 25 kg/s for production is set as the base case for subsequent analysis.

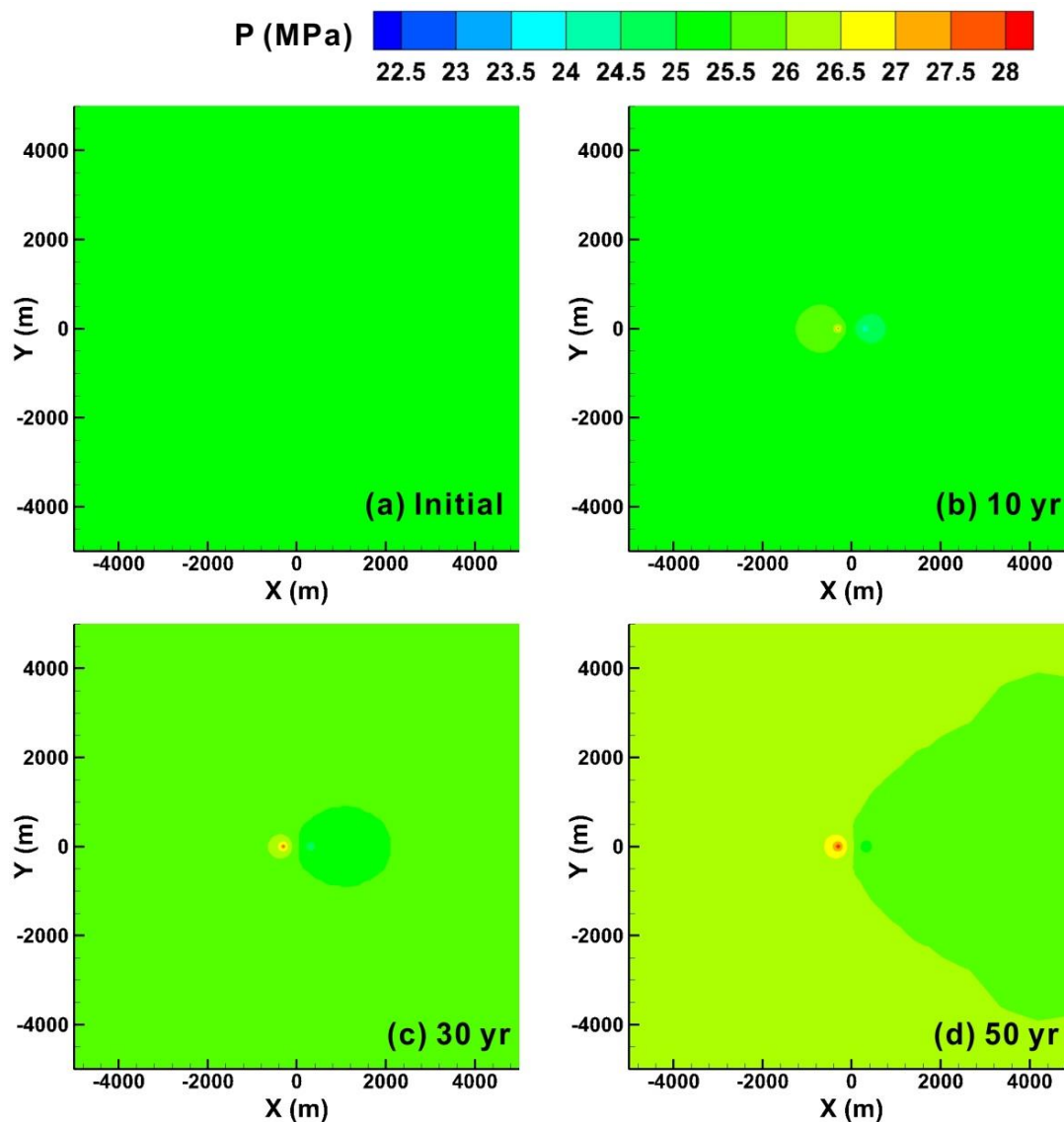


Figure 3. The reservoir pressure distribution at different times with the scheme of the different mass flow rate for injection (27.5 kg/s) and production (25.0 kg/s).

The temperature distribution in the reservoir at different times is shown in Figure 4. The temperature at the bottom of the production well is about 337 °C, which has dropped by 163 °C (32.6%) in 50 years. It is worth noting that according to the past development experience of the traditional geothermal system, the temperature drop should be regulated within 10 °C during the operation period [24]. Otherwise, the thermal breakthrough will pose a threat to the sustainability of the system. However, it may not be suitable for the supercritical geothermal system. Although it experienced a considerable drop, the temperature is still high enough for future utilization.

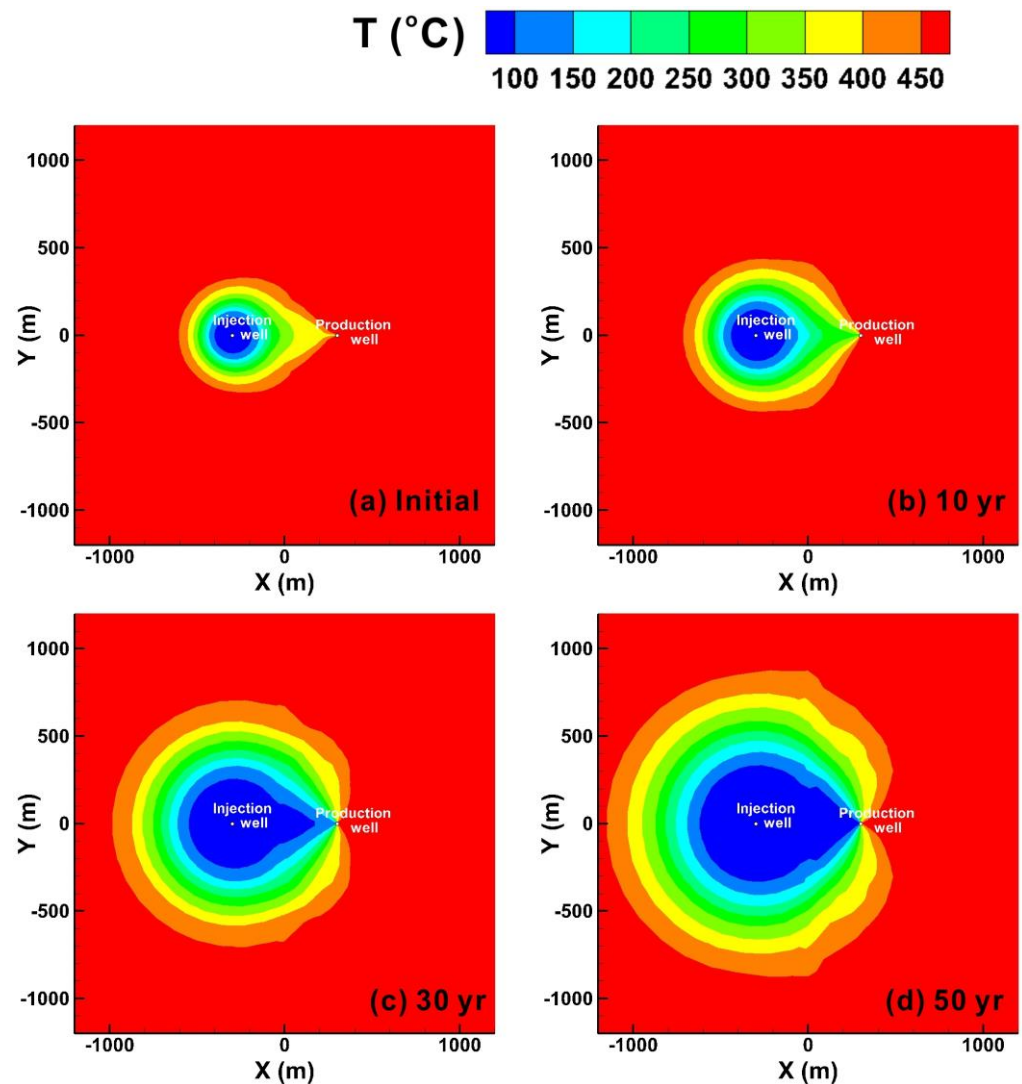


Figure 4. The reservoir temperature distribution at different times.

3.1.2. Evolution in the Production Well

Figure 5 shows the evolution of temperature, pressure, and steam saturation at the production wellhead over 50 years. The whole operation could be approximately divided into three stages according to the temperature evolution. The first is a stable stage from 0 to 4 years, during which the producing fluid presents in steam, with a temperature of 415 °C at the wellhead. Subsequently, it reaches a plummet stage, lasting about 1.2 years, with the temperature dropping to 342 °C. The reason for this is that the injected cold water reaches the production well in a two-phase state. The relatively low pressure at the production well bottom corresponds to a low saturation temperature, which is far lower than the in-situ temperature. At the same time, because of the higher mobility (defined as ρ/μ) of the liquid than the steam phase, a smaller pressure difference at the well bottom can maintain the fixed mass flux. Hence, there occurs an increase in the pressure. This is followed by the third stage, where the producing fluid turns into the two-phase state, and the temperature and pressure continue decreasing gradually and simultaneously until the end of the operation.

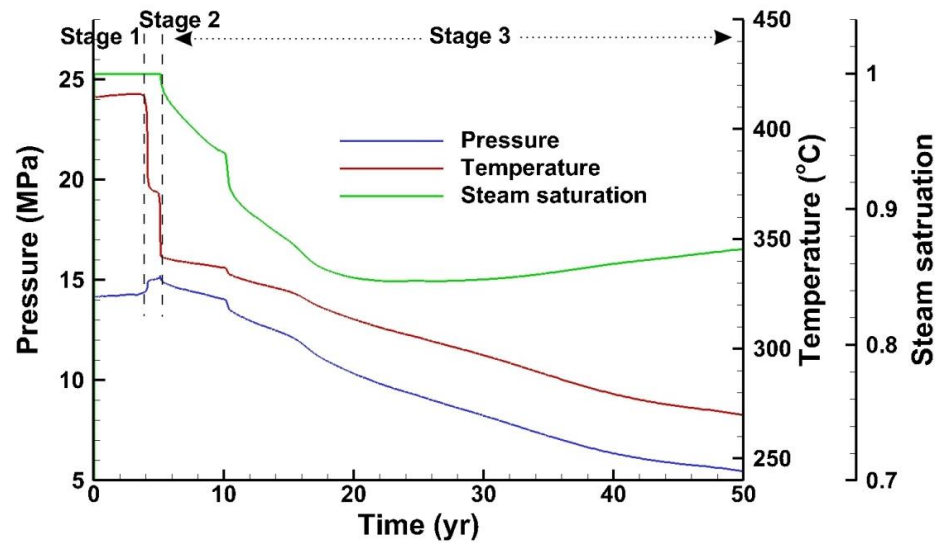


Figure 5. The evolution of pressure, temperature, and steam saturation at the production wellhead.

The production fluid in supercritical geothermal systems experiences a complicated phase transition process, which differs from the traditional ones. In Stages 1 and 2 (0~5.5 years), the production fluid presents in steam. When the fluid flows upward from the production well bottom to the wellhead, even though the pressure drops below the critical pressure, the high in-situ temperature of the reservoir ensures that the P-T profile along the wellbore does not intersect with the saturation line. Thus, the fluid transits directly from the supercritical phase to steam. After 5.5 years of operation, the cold front in the reservoir expands toward the production well, which cools the reservoir, making the P-T profile fall on and evolve along the saturation line. Hence, the outflow transit to a water-steam mixture. After about 15 years, the bottom transits to the liquid state totally (Figure 6a). When the fluid flows upward, the decrease in pressure makes part of the liquid transit to steam and form a two-phase mixture at the wellhead.

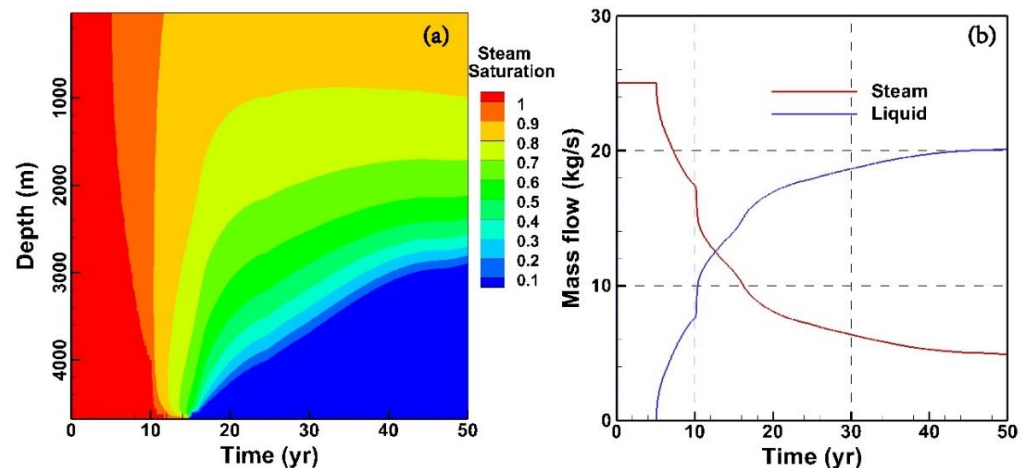


Figure 6. Gas saturation distribution in production well (a) and the production mass flow rate in different phases (b).

In addition, following the continuous decrease of the reservoir temperature, the steam saturation of the production fluid also gradually decreased, dropping to a minimum of 0.85 in 20 years (Figure 5). Although there is a slight increase in the steam saturation after 20 years, the mass flux in the steam phase keeps decreasing since the two-phase fluid occurs; it is only 5 kg/s, accounting for about 20% in total (Figure 6b). If the system runs

long enough, the production fluid will eventually exist only in a liquid phase, which is more like a conventional thermal reservoir.

3.2. Heat Extraction Performance

3.2.1. Heat Production Rate and Power Generation Efficiency

The variation in net heat flow (W_h) and power generation (W_e) for 50 years is shown in Figure 7a, sharing a similar evolutionary pattern. The values of W_h and W_e maintain 70.0 MW and 16.2 MW. Compared with the temperature evolution, the evolution of net heat flow and power generation looks smoother, without a distinct boundary between Stages 2 and 3. The values of W_h and W_e drop to 57.5 MW/11.8 MW and 31.0 MW/5.4 MW at the end of Stages 2 and 3, respectively. The conversion efficiency (f) is the ratio of power generation to the net heat flow, which considers the two processes from thermal to mechanical and then to power, and positively strictly relates to the outflow temperature. Such a high temperature brings a high efficiency of over 0.23 when the fluid presents in the single-steam phase. Then, it decreases with the temperature to 0.174 at the end of the operation.

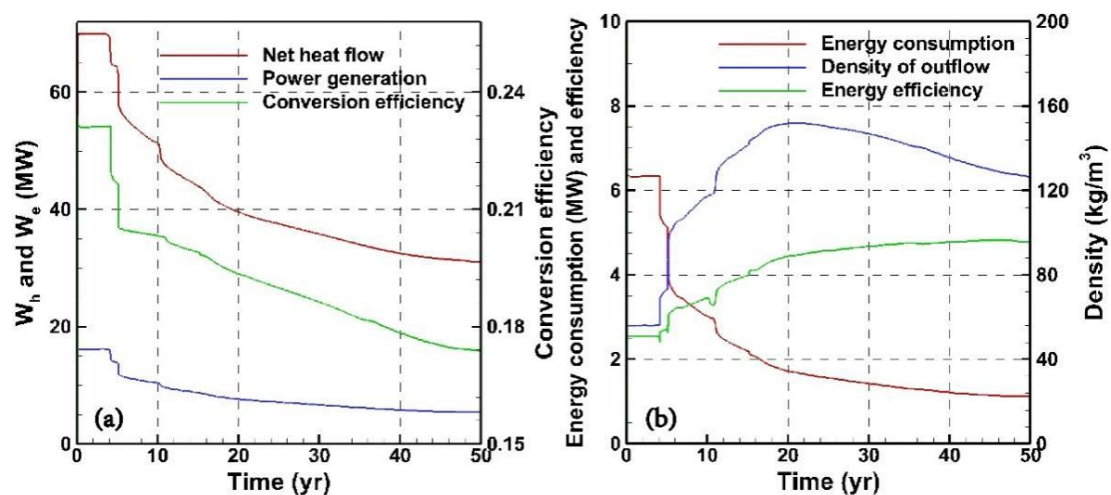


Figure 7. The evolution of net heat flow (W_h), power generation (W_e), and conversion efficiency (f) (a); and energy consumption, energy efficiency, and density of outflow (b).

3.2.2. Energy Consumption of Pump and Energy Efficiency

Applying pressure at the wellhead is the main reason for the energy consumption of the pump. For the injection well, the reservoir is located at a depth of about 4500 m with a temperature of 500 °C. Assuming the injection well is filled with cold water with a density of over 950 kg/m³, the pressure at the injection well bottom could reach 42 MPa, far higher than the in-situ pressure. Hence, the recharged fluid could flow into the reservoir spontaneously without any pressurization at the wellhead.

The blue line in Figure 7b shows the evolution of energy consumption in the production well. According to Equation (5), the pump's energy consumption positively relates to the wellhead pressure and negatively to the fluid density. In Stages 1 and 2, the production well is filled with low-density high-temperature steam, which results in high energy consumption and low energy efficiency. In Stage 3, the fluid density in the wellbore increases with the decrease in temperature and steam saturation. Thus, the pressure at the wellhead decreases, lowering the energy consumption and increasing energy efficiency.

3.3. Effects of Mass Flow Rate on Production Performance

3.3.1. Mass Flow Rate

For realistic geothermal engineering, the injection and production flow rate greatly affect the performance and sustainability of the geothermal system. A higher mass flow

rate will bring better heat extraction performance, but it also implies an earlier thermal breakthrough, influencing the system's sustainability. It is significant to determine a proper mass flow rate for any geothermal system. The production flow rate in the base case is 25 kg/s. Here, two cases with higher (35 kg/s) and lower (15 kg/s) mass flow rates are given for discussion. For both cases, the injection mass flow rate is set as 10% higher than the production.

The net heat flow of the three cases keeps proportional to the mass flow rate during the operation; as shown in Figure 8, a higher rate corresponds to a shorter Stage 1. Meanwhile, the conversion efficiency (f) negatively relates to the mass flow rate, even in the single-steam phase stage (Stage 1). The reason is that the higher rate corresponds to a lower pressure at the production well bottom and a larger frictional pressure loss along the wellbore, i.e., a lower production pressure at the wellhead. According to the Joule–Thomson effect, the pressure keeps proportional to the temperature during an approximately isenthalpic process. When it comes to the late stage, the fluid in higher rate cases could not be heated enough as in the lower cases. Thus, the conversion efficiency negatively relates to the mass flow rate, and the power generation of the 35 kg/s case is close to the base case at the end of the operation (6.2 MW vs. 5.4 MW). Hence, the sustainability of a geothermal system is decided by the reservoir's characteristics, such as size and permeability distribution. For the present case, with a well spacing of 600 m, 35 kg/s nearly reaches the maximum for a sustainability of 50 years.

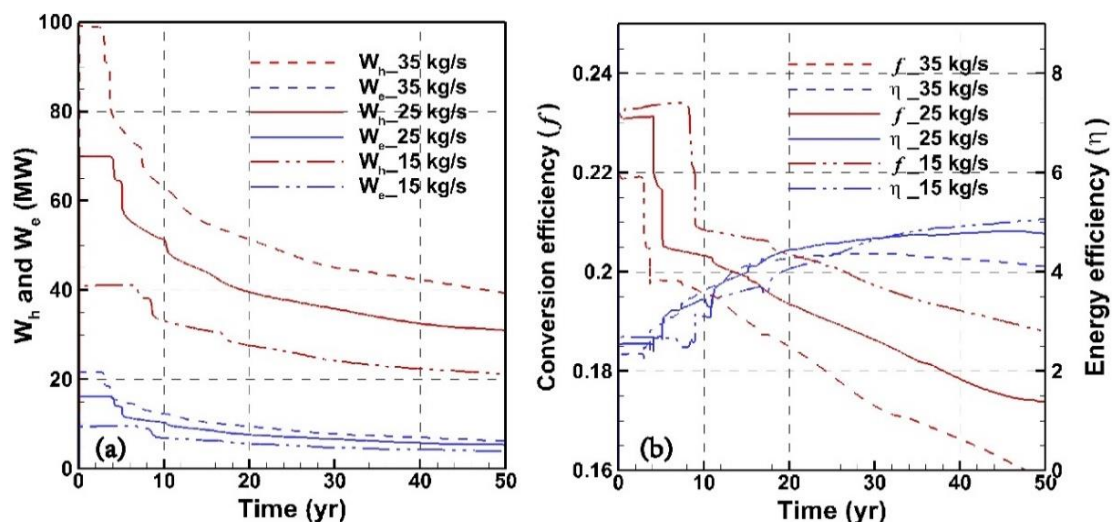


Figure 8. The evolution of net heat flow (W_h), power generation (W_e) (a), and conversion efficiency and energy efficiency (b) with different flow rates.

3.3.2. Reservoir Permeability

Permeability is critical for assessing the potential of a geothermal system [25–28]. Many factors will affect the permeability distribution of the reservoir, such as the local stress conditions, natural fractures, reservoir lithology, and fluid chemical composition. Moreover, the reservoir is stimulated by cold water and gets an excellent result [6]. Multiple factors contribute to the uncertainty of the reservoir's permeability distribution. Therefore, a lower (25 mD) and a higher (100 mD) permeability case with other parameters unchanged are given to study the influence of different permeabilities.

Because of the same mass flow rate, the W_h evolution of the three cases almost overlaps perfectly. In comparison, higher permeability means higher pressure at the production well bottom. A weaker J-T effect brings a higher temperature at the wellhead and conversion efficiency, as shown by the red lines in Figure 9b. The minor difference in conversion efficiency causes a slight difference in power generation. In addition, under the combined effect of the pressure and fluid density at the wellhead, a higher permeability brings a

higher energy efficiency (η). It can be drawn that for the mass flow under the scheme of fixed injection-production rate, the permeability has a minor influence on the heat extraction performance in some certain range. If the permeability is low enough, the pump should even be assembled in the production well to help extract the fluid. The flow rate should be elaborately regulated according to the wellhead pressure.

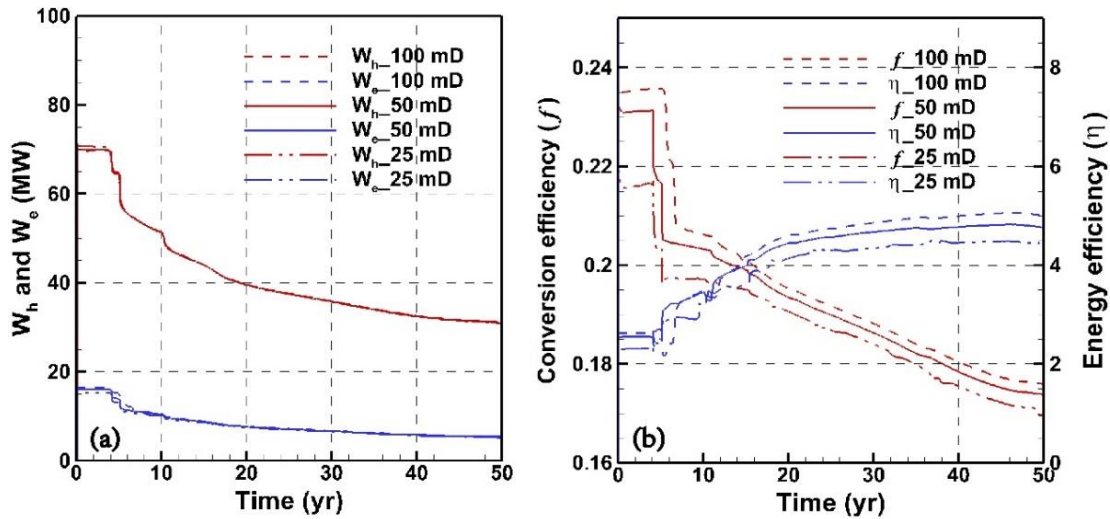


Figure 9. The evolution of net heat flow (W_h), power generation (W_e) (a), and conversion efficiency and energy efficiency (b) with different reservoir permeabilities.

3.3.3. Well Spacing

The well spacing determines the time of thermal breakthrough and the sustainability of the system; a large well spacing is conducive for a long lifetime, but the unknown connectivity between wellbores is a potential threat. There is only one borehole for the IDDP-2 project. The location of the second well has not been decided. Here, different well spacing is given to provide a guide. The cases include 400 m, 600 m (base case), and 800 m. The results are shown in Figure 10.

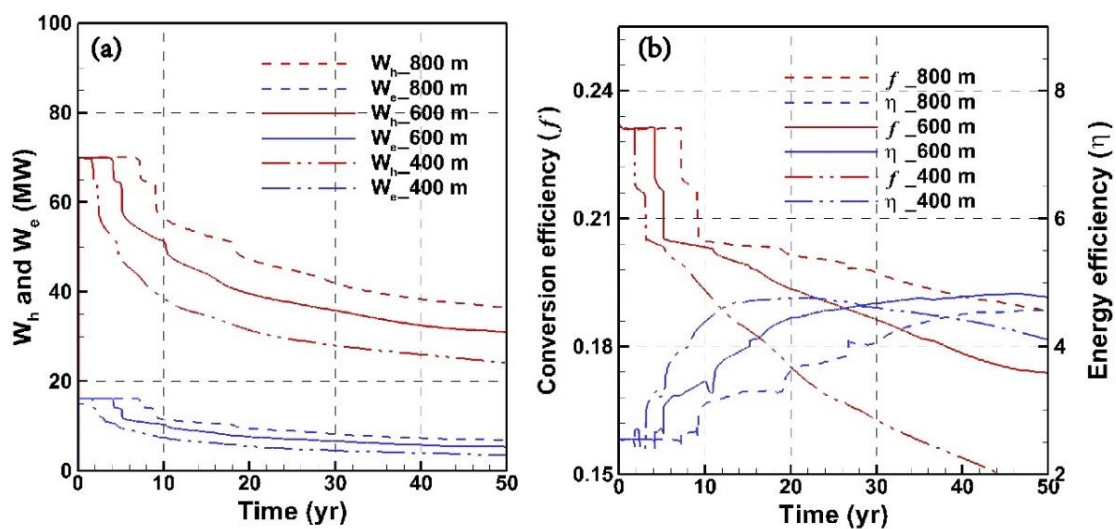


Figure 10. The evolution of net heat flow (W_h), power generation (W_e) (a), and conversion efficiency and energy efficiency (b) with different well spacing.

It can be seen from Figure 10 that the duration of the single-steam phase stage (Stage 1) increases significantly with the well spacing, as well as the net heat flow (W_h) and power

generation (W_e) in the late stage. The main reason for this is that as the well spacing increases, there is a larger room for the fluid to absorb heat from the reservoir. The conversion efficiency shares a similar evolutionary tendency with the net heat flow. However, the evolution of energy efficiency is not monotonous. In the first 30 years, the energy efficiency negatively relates to the well spacing, but only in the small well spacing case, the efficiency decreases with time. The reason is that the efficiency is decided by both pressure and fluid density; at the same time, fluid density is affected by pressure and temperature. Thus, the energy efficiency is also a function of the wellhead pressure, which needs to be elaborately regulated in practical engineering.

4. Discussion

4.1. Economic Analysis

The construction of geothermal power plants generally involves the following steps: (1) preliminary geological, hydrogeological, and geothermal geological surveys; (2) drilling; (3) reservoir reconstruction; (4) construction of a geothermal fluid circulation system; (5) construction of ground power generation equipment; and (6) installation of transmission lines [23,29,30]. At present, the power generation plant well mainly includes the following aspects: (1) drilling; (2) reservoir reconstruction; (3) surface power generation equipment installation; and (4) operation and maintenance.

Since there is no related report after the well is completed, the cost before drilling is estimated to be 14~16 million dollars (www.iddp.is, accessed on 20 December 2020). Regarding the cost of the reservoir reconstruction part, although the supercritical geothermal system has a higher temperature, the hot stimulation effect during hydraulic fracturing is better. The mechanical properties of the rock have changed under the influence of high temperature and high-pressure conditions; it is the transformation from brittle rock to plastic rock. After fracturing, most of the open cracks may recover naturally, so special proppants are required for operation. The cost of reservoir reconstruction for a traditional geothermal system is about 0.5 million dollars [28], while the cost of a supercritical geothermal system is assumed to be 2 million dollars. In terms of surface power generation equipment, since there is a power plant in the Reykjanes geothermal field and the IDDP-2 well continues to be drilled based on the RN-15 well, the cost of this part is negligible. Operation and maintenance costs include system energy consumption, personnel, insurance costs, and so on. Figure 11 shows the energy consumption of the pump for 50 years and it reaches 950.09 GWh. The price of industrial electricity in Iceland in 2021 is 0.051 \$/kWh, and the cost of internal energy consumption is 48.45 million dollars, combined with other consumption for a total of 55 million dollars.

In summary, the total cost of the supercritical geothermal power station in the Reykjanes geothermal field is 72 million dollars. The main impact on the total cost is the operation and maintenance costs. The levelized cost of electricity (LCOE) is the most commonly used indicator for evaluating the economic feasibility of a power generation system [28,30,31]. It is the ratio of the total cost of the power station system to the total power generation in 50 years. In this study, the 50-year average installed capacity of the proposed supercritical power station is 8.13 MW, and the total power generation is 3551 GWh. Therefore, the LCOE is approximately 0.02 \$/kWh, which is much lower than the commercial electricity price in Iceland. Therefore, the supercritical geothermal resources of the Reykjanes geothermal field have great development and utilization value.

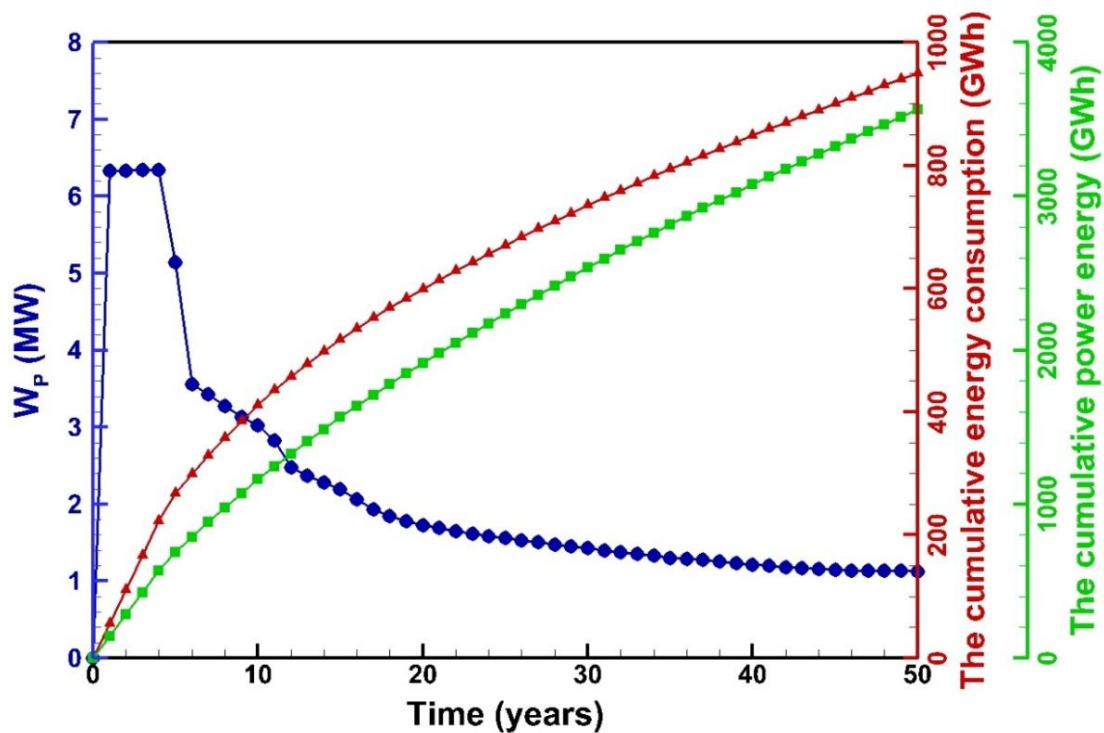


Figure 11. Evolution of the internal energy consumption and the cumulative energy consumption of the production pumps in 50 years lifetime.

4.2. Environmental Benefits

As a type of clean energy, supercritical geothermal resources can greatly reduce the CO₂ emissions from fossil fuels. According to previous research experience, the greenhouse gas emissions of geothermal power plants are about 122 g/kWh, while the emissions of traditional power plants are 460~1290 g/kWh [23,28]. The power station proposed in this study can reduce 1.2~7.75 Mt of greenhouse gases in 50 years, which also shows the importance of alleviating the greenhouse effect.

At the same time, there are many problems in the development of supercritical geothermal resources: (1) the change of supercritical temperature and pressure conditions of the salt-containing fluid; (2) the blockage of the reservoir that may be caused by the injection fluid, etc. The authors will continue this research in follow-up works.

5. Conclusions

In this study, a doublet supercritical geothermal system is simulated based on IDDP-2 in Reykjanes for thermal energy extraction. The favorable conditions for operation are discussed, and an economic analysis is conducted. According to the simulation results, the following conclusions can be drawn:

1. The fluid existing in the supercritical state behaves like a gas. The injected cold water makes the fluid condensed and brings a constant decrease in pressure. A compensatory injection-production scheme is needed for supercritical geothermal development to maintain the reservoir pressure and sustainability.
2. The pressure at the production wellhead is the main reason for the pump's energy consumption. However, extremely low pressure decreases the fluid's density, also increasing energy consumption. Moreover, it will cool the production fluid and lower the conversion efficiency. It is a dilemma for the schematic design and needs more optimization work.
3. The LCOE assessment is 0.02 \$/kWh, which is lower than the commercial electricity price in Iceland, and it reduces greenhouse gas emissions by 1.2~7.75 Mt compared with traditional power plants. According to the comprehensive analysis of economic

and environmental benefits, the proposed power plant has greater development and utilization value.

Author Contributions: Conceptualization, T.X. and G.F.; methodology, G.F. and Y.W.; software, G.F.; validation, G.F. and Y.W.; formal analysis, G.F. and Y.W.; investigation, Y.W. and G.F.; resources, Y.W.; data curation, Y.W.; writing—original draft preparation, Y.W.; writing—review and editing, T.X., G.F. and Y.C.; visualization, Y.W., Y.C. and G.F.; supervision, T.X.; project administration, T.X.; funding acquisition, T.X. and G.F. All authors have read and agreed to the published version of the manuscript.

Funding: This research was funded by the National Natural Science Foundation of China, grant numbers 41902309 and 42130303. This research has also been funded by the Engineering Research Center of Geothermal Resources Development Technology and Equipment, Ministry of Education, Jilin University.

Data Availability Statement: The data on IDDP-2 could be found on the website “<https://iddp.is/wp-content/uploads/2017/02/IDDP-2-Completion-websites-IDDP-DEEPEGS2.pdf>, accessed on 10 February 2017”.

Conflicts of Interest: The authors declare no conflict of interest.

Nomenclature

W_h	Net heat production rate, W
h_{pro}	Production specific enthalpy, J/kg
f_1	Conversion efficiency, from thermal to mechanical energy
f	Conversion efficiency, from thermal to electrical energy
W_{p1}	Energy consumption of injection pump, W
T_{inj}	Injection temperature, °C
η_e	Energy efficiency
q_{inj}	Injection mass flow rate, kg/s
ρ	fluid density, kg/m ³
W_e	Electric power, W
h_{inj}	Injection specific enthalpy, J/kg
f_2	Conversion efficiency, from mechanical to electrical energy
Q_{pro}	Water production rate, kg/s
W_{p2}	Energy consumption of production pump, W
T_{pro}	Production temperature, °C
η_p	Pump efficiency
q_{pro}	Production mass flow rate, kg/s
P	Pressure, MPa

References

- Dai, Z.; Xu, L.; Xiao, T.; McPherson, B.; Zhang, X.; Zheng, L.; Dong, S.; Yang, Z.; Soltanian, M.R.; Yang, C.; et al. Reactive chemical transport simulations of geologic carbon sequestration: Methods and applications. *Earth-Sci. Rev.* **2020**, *208*, 103265. [CrossRef]
- Reinsch, T.; Dobson, P.; Asanuma, H.; Huenges, E.; Poletto, F.; Sanjuan, B. Utilizing supercritical geothermal systems: A review of past ventures and ongoing research activities. *Geotherm. Energy* **2017**, *5*, 16. [CrossRef]
- Friðleifsson, G.O.; Elders, W.A. The Iceland Deep Drilling Project: A search for deep unconventional geothermal resources. *Geothermics* **2005**, *34*, 269–285. [CrossRef]
- Friðleifsson, G.O.; Elders, W.A.; Albertsson, A. The concept of the Iceland deep drilling project. *Geothermics* **2014**, *49*, 2–8. [CrossRef]
- Friðleifsson, G.Ó.; Elders, W.A.; Zierenberg, R.A.; Stefánsson, A.; Fowler, A.P.; Weisenberger, T.B.; Harðarson, B.S.; Mesfin, K.G. The Iceland Deep Drilling Project 4.5 km deep well, IDDP-2, in the seawater-recharged Reykjanes geothermal field in SW Iceland has successfully reached its supercritical target. *Sci. Drill.* **2017**, *23*, 1–12. [CrossRef]
- Friðleifsson, G.Ó.; Elders, W.A.; Zierenberg, R.A.; Fowler, A.P.G.; Weisenberger, T.B.; Mesfin, K.G.; Sigurðsson, Ó.; Niélsson, S.; Einarsson, G.; Óskarsson, F.; et al. The Iceland Deep Drilling Project at Reykjanes: Drilling into the root zone of a black smoker analog. *J. Volcanol. Geotherm. Res.* **2020**, *391*, 106435. [CrossRef]
- Saemundsson, K.; Sigurgeirsson, M.A.; Friðleifsson, G.O. Geology and structure of the Reykjanes volcanic system, Iceland. *J. Volcanol. Geotherm. Res.* **2020**, *391*, 106501. [CrossRef]

8. Friðleifsson, G.Ó.; Elders, W.A. Successful drilling for supercritical geothermal resources at Reykjanes in SW Iceland. *GRC Trans.* **2017**, *41*, 1095–1107.
9. Zierenberg, R.A.; Fowler, A.P.; Friðleifsson, G.Ó.; Elders, W.A.; Weisenberger, T.B. Preliminary description of rocks and alteration in IDDP-2 drill core samples recovered from the Reykjanes Geothermal System, Iceland. *GRC Trans.* **2017**, *41*, 1599–1615.
10. Cladouhos, T.T.; Petty, S.; Bonneville, A.; Schultz, A.; Sorlie, C.F. Super hot EGS and the Newberry deep drilling project. In Proceedings of the 43rd Workshop on Geothermal Reservoir Engineering, Stanford University, Stanford, CA, USA, 12–14 February 2018; Stanford University: Stanford, CA, USA, 2018.
11. Feng, G.; Wang, Y.; Xu, T.; Shi, Y. Multiphase flow modeling and energy extraction performance for supercritical geothermal systems. *Renew. Energy* **2021**, *173*, 442–454. [[CrossRef](#)]
12. Feng, G.; Xu, T.; Zhao, Y.A.; Gherardi, F. Heat mining from super-hot horizons of the Larderello geothermal field, Italy. *Renew. Energy* **2022**, *197*, 371–383. [[CrossRef](#)]
13. Feng, Y.; Chen, L.; Suzuki, A.; Kogawa, T.; Okajima, J.; Komiya, A.; Maruyama, S. Enhancement of gas production from methane hydrate reservoirs by the combination of hydraulic fracturing and depressurization method. *Energy Convers. Manag.* **2019**, *184*, 194–204. [[CrossRef](#)]
14. Yu, T.; Guan, G.; Abudula, A.; Yoshida, A.; Wang, D.; Song, Y. Heat-assisted production strategy for oceanic methane hydrate development in the Nankai Trough, Japan. *J. Pet. Sci. Eng.* **2019**, *174*, 649–662. [[CrossRef](#)]
15. Luo, F.; Xu, R.-N.; Jiang, P.-X. Numerical investigation of fluid flow and heat transfer in a doublet enhanced geothermal system with CO₂ as the working fluid (CO₂-EGS). *Energy* **2014**, *64*, 307–322. [[CrossRef](#)]
16. Hokstad, K.; Tanavsuu-Milkeviciene, K. Temperature Prediction by Multigeophysical Inversion: Application to the IDDP-2 Well at Reykjanes, Iceland. *GRC Trans.* **2017**, *41*, 1033790.
17. Guo, T.; Tang, S.; Sun, J.; Gong, F.; Liu, X.; Qu, Z.; Zhang, W. A coupled thermal-hydraulic-mechanical modeling and evaluation of geothermal extraction in the enhanced geothermal system based on analytic hierarchy process and fuzzy comprehensive evaluation. *Appl. Energy* **2020**, *258*, 113981.1–113981.12. [[CrossRef](#)]
18. Hu, Z.; Xu, T.; Feng, B.; Yuan, Y.; Li, F.; Feng, G.; Jiang, Z. Thermal and fluid processes in a closed-loop geothermal system using CO₂ as a working fluid—ScienceDirect. *Renew. Energy* **2020**, *154*, 351–367. [[CrossRef](#)]
19. Liang, X.; Xu, T.; Feng, B.; Jiang, Z. Optimization of heat extraction strategies in fault-controlled hydro-geothermal reservoirs. *Energy* **2018**, *164*, 853–870. [[CrossRef](#)]
20. Pruess, K. Enhanced geothermal systems (EGS) using CO₂ as working fluid—A novel approach for generating renewable energy with simultaneous sequestration of carbon. *Geothermics* **2006**, *35*, 351–367. [[CrossRef](#)]
21. Sanyal, S.K.; Butler, S.J. An analysis of power generation prospects from enhanced geothermal systems. *Geotherm. Resour. Counc. Trans.* **2005**, *29*, 131–138.
22. Zeng, Y.C.; Su, Z.; Wu, N.Y. Numerical simulation of heat production potential from hot dry rock by water circulating through two horizontal wells at Desert Peak geothermal field. *Energy* **2013**, *56*, 92–107. [[CrossRef](#)]
23. Xu, T.; Yuan, Y.; Jia, X.; Lei, Y.; Li, S.; Feng, B.; Hou, Z.; Jiang, Z. Prospects of power generation from an enhanced geothermal system by water circulation through two horizontal wells: A case study in the Gonghe Basin, Qinghai Province, China. *Energy* **2018**, *148*, 196–207. [[CrossRef](#)]
24. Panel, M.L. The Future of Geothermal Energy. Impact of Enhanced Geothermal Systems [EGS] on the United States in the 21st century. *Geothermics* **2006**, *17*, 881–882.
25. Zeng, Y.C.; Zhan, J.M.; Wu, N.Y.; Luo, Y.Y.; Cai, W.H. Numerical simulation of electricity generation potential from fractured granite reservoir through a single horizontal well at Yangbajing geothermal field. *Energy* **2016**, *103*, 290–304. [[CrossRef](#)]
26. Chen, Y.; Ma, G.; Wang, H.; Li, T.; Wang, Y. Application of carbon dioxide as working fluid in geothermal development considering a complex fractured system. *Energy Convers. Manag.* **2018**, *180*, 1055–1067. [[CrossRef](#)]
27. Song, X.; Yu, S.; Li, G.; Yang, R.; Lyu, Z. Numerical simulation of heat extraction performance in enhanced geothermal system with multilateral wells. *Appl. Energy* **2018**, *218*, 325–337. [[CrossRef](#)]
28. Zhang, Y.-J.; Li, Z.-W.; Guo, L.-L.; Gao, P.; Jin, X.-P.; Xu, T.-F. Electricity generation from enhanced geothermal systems by oilfield produced water circulating through reservoir stimulated by staged fracturing technology for horizontal wells: A case study in Xujiaweizi area in Daqing Oilfield, China. *Energy* **2014**, *78*, 788–805. [[CrossRef](#)]
29. Chen, J.; Jiang, F. Designing multi-well layout for enhanced geothermal system to better exploit hot dry rock geothermal energy. *Renew. Energy* **2015**, *74*, 37–48. [[CrossRef](#)]
30. Cui, G.; Pei, S.; Rui, Z.; Dou, B.; Ning, F.; Wang, J. Whole process analysis of geothermal exploitation and power generation from a depleted high-temperature gas reservoir by recycling CO₂. *Energy* **2021**, *217*, 119340. [[CrossRef](#)]
31. Yuan, F.; Xi, C.; Xi, F.X. Current status and potentials of enhanced geothermal system in China: A review. *Renew. Sustain. Energy Rev.* **2014**, *33*, 214–223.